EtNHMe, 624-78-2; $H_2N(CH_2)_2NH_2$, 107-15-3; NH_2OH, 7803-49-8; NH_2CH_2OH, 3088-27-5; $NH_2CH_2CH_2OH$, 141-43-5; MeN=NH, 26981-93-1; MeN=NMe, 503-28-6; N_2C=NH, 2053-29-4; H_3CCH=NH, 20729-41-3; H_2C=NMe, 1761-67-7; MeCH=NMe, 6898-67-5; H_2C=NOH, 75-17-2; MeN=O, 865-40-7; MeCHO, 75-07-0; MeCOMe, 67-64-1; $MeCH=CH_2$, 115-07-1; $H_2NCH=CH_2$, 593-67-9; H_2NCH=NH, 463-52-5; NH_2CHO, 75-12-7; NH_2COMe, 60-35-5; $CH_2(OH)_2$, 463-57-0.

Magnetic Circularly Polarized Luminescence of Zinc Phthalocyanine in an Argon Matrix

David H. Metcalf,[†] Thomas C. VanCott,[†] Seth W. Snyder,[‡] Paul N. Schatz,*[,†]

Chemistry Department and Biophysics Program, University of Virginia, McCormick Road, Charlottesville, Virginia 22901

and Bryce E. Williamson

Chemistry Department, University of Canterbury, Christchurch 1, New Zealand *(Received: July 19, 1989; In Final Form: October 16, 1989)*

The magnetic circularly polarized luminescence (MCPL) of the Q transition of zinc phthalocyanine has been measured in an argon matrix. These are the first such measurements for a matrix-isolated sample and support previous interpretations that require a crystal-field-stabilized Jahn-Teller splitting in the $^1E_u(\pi^*)$ excited state. A moment analysis indicates the presence of a Ham effect which reduces the orbital angular momentum of this state by about 30%. Energy transfer between inequivalent sites in the matrix results in a red shift of the emission relative to the Q(0,0) absorption band.

Introduction

Recently we reported detailed absorption and magnetic circular dichroism (MCD) spectra of zinc phthalocyanine in an argon matrix (ZnPc/Ar) between 14 700 and 74 000 cm^{-1}.[1] (See ref 1 and references therein for recent reviews of the spectroscopic literature on Pc's.) The lowest energy allowed transition of ZnPc, at ~15 200 cm^{-1}, is designated the Q transition and in D_{4h} symmetry corresponds to $^1A_{1g}(\pi) \rightarrow {}^1E_u(\pi^*)$.

MCD[1] and emission studies[2] have shown that the degeneracy of the Q state is lifted in a matrix, probably as a result of a crystal-field-stabilized Jahn-Teller effect.[1,2] One of the consequences of this splitting is that the magnetic circularly polarized luminescence (MCPL) from the Q state should consist purely of negative $\mathcal{B}$ terms (see later).

In this work, we report the emission and MCPL of ZnPc/Ar obtained using a sensitive CPL spectrometer that was designed by one of us (D.H.M.) and built at the University of Virginia. We believe that these are the first reported measurements of MCPL from a matrix-isolated sample.

Experimental Section

The full procedure for matrix deposition has been described previously.[1,3] The ZnPc, purified as previously described,[1] was sublimed at ~340°C and codeposited with argon on a cryogenically cooled (~5 K) sapphire window in the bore of a superconducting coil. The initial spectra were unresolved, the Q(0,0) band consisting of a single almost symmetrical absorption contour of ~75 cm^{-1} fwhm accompanied by a corresponding single positive $\mathcal{A}$ term. However, annealing the spectra for a few minutes at ~20 K produced a dramatic sharpening with the emergence of perhaps 10 distinct sites (solid curves, Figures 1 and 2). The spectra are quite similar to those obtained in our earlier study (ref 1, Figure 5) but are even more clearly resolved.

MCD and double-beam absorption spectra were obtained simultaneously using a spectrometer that has been described earlier.[4,5] The magnetic field strength and spectral resolution were respectively 0.37 T and 0.15 nm. The depolarization of circularly polarized light due to the sample was found to be negligible by comparing the natural CD of a solution of Λ-tris(1,2-ethanediamine)cobalt(III) inserted after the sample with that of the same solution in the absence of the sample.

The total luminescence (TL) and the MCPL were measured with an instrument that will be described in detail later.[6] Emission was excited with 488-nm radiation from an argon ion laser (Coherent Radiation CR-5) which was focused to a slit image at the sample. The emitted light was collected at 180° to the incident beam and passed through a fused-quartz photoelastic modulator and a 570-nm glass cutoff filter to the entrance slit of a 3/4-m double monochromator (Spex 1400-2). The spectral resolution was 0.3 nm. The luminescence was detected in photon-counting mode by using a cooled photomultiplier tube with S-20 response. The MCPL was determined with a laboratory-built gated photon counting device referenced to the photoelastic modulator.[6] The MCPL measurements were made at a field strength of 3.00 T and at a temperature of ~5 K.

Results

The spectra over the full range of the Q-band region are illustrated in Figure 1. The absorption (A) and MCD (ΔA) spectra (solid lines) are respectively compared with the TL (I) and MCPL (ΔI) shown by the dashed lines.

Three major band envelopes are observed in absorption. These are denoted Q(0,0), Q(1,0) and Q(2,0) in Figure 1. Q(0,0) comprises the zero-phonon bands of several sites.[1] Q(1,0) and Q(2,0) contain contributions from overlapping vibronic bands,[1,2] but Q(2,0) also contains a contribution from a separate electronic transition.[1,2]

To the red of the Q(0,0) region in emission are two band envelopes, at ~14 500 and ~13 700 cm^{-1} (Figure 1). These contain vibronic bands associated with the Q transition of ZnPc[1,2] but also contain a substantial contribution due to small amounts of H_2Pc impurity, as has been observed by previous workers.[2]

[†] Chemistry Department, University of Virginia.
[‡] Biophysics Program, University of Virginia.

(1) VanCott, T. C.; Rose, J. L.; Misener, G. C.; Williamson, B. E.; Schrimpf, A. E.; Boyle, M. E.; Schatz, P. N. *J. Phys. Chem.* **1989**, *93*, 2999.
(2) Huang, T. H.; Rieckhoff, K. E.; Voigt, E. M. *J. Chem. Phys.* **1982**, *77*, 3424.
(3) Lund, P. A.; Smith, D.; Jacobs, S. M.; Schatz, P. N. *J. Phys. Chem.* **1984**, *88*, 31.
(4) Rose, J.; Smith, D.; Williamson, B. E.; Schatz, P. N.; O'Brien, M. C. M. *J. Phys. Chem.* **1986**, *90*, 2608.
(5) Misener, G. C. Ph.D. Dissertation, University of Virginia, Charlottesville, VA, 1987.
(6) Metcalf, D. H.; Cummings, W. J.; Richardson, F. S. To be published.

0022-3654/90/2094-2828$02.50/0

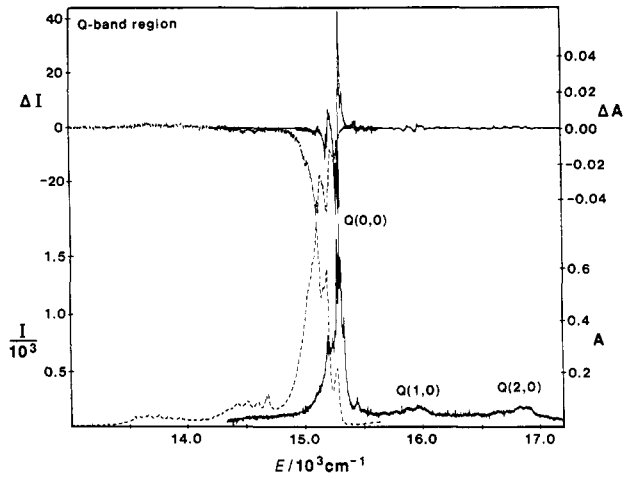

Figure 1. Spectra of ZnPc/Ar in the Q-band region. The upper and lower dashed curves are respectively the MCPL per tesla and total luminescence (TL) in photon counts, and the upper and lower solid curves are the MCD (per tesla) and absorption in optical density units. The strong bands labeled Q(0,0) correspond to zero-phonon transitions from several sites in the Ar host. Q(1,0) and Q(2,0) contain vibronic bands built on Q(0,0), but Q(2,0) also contains a separate electronic transition.[1,2] The emission envelopes at ~14 500 and 13 700 cm^{-1} contain vibronic bands as well as emission bands from H_2Pc impurity sites.

The Q(0,0) region is illustrated in greater detail in Figure 2. The emission spectra are shifted to the red in relation to the absorption and MCD. Whereas the MCD shows both positive and negative bands, the MCPL shows only negative bands.

Discussion

The MCD and MCPL are respectively defined by eqs 1 and 2.[7]

$$\Delta A' = A'_L - A'_R \tag{1}$$

$$\Delta I' = I'_L - I'_R \tag{2}$$

The subscripts L and R indicate the absorption or emission of left or right circularly polarized light, respectively, and the primes indicate magnetic field dependent quantities.

Let us consider a fully allowed electronic transition between Born–Oppenheimer states A and J. In designating transitions, for example, A → J, J ← A, etc., we follow the convention[7] that the state on the left is always the lower energy state, so the direction of the arrow distinguishes absorption and emission. We have previously shown that in ZnPc/Ar the molecules show strong selective orientation with the planar rings parallel to the deposition window.[1] Then in the rigid shift approximation[1,7]

$$\frac{\Delta A'}{\mathcal{E}} = \gamma\mu_B B\left[\mathcal{A}_1^z(\mathrm{A}\rightarrow\mathrm{J})\left(\frac{-\partial f(\mathcal{E})}{\partial\mathcal{E}}\right) + \left(\mathcal{B}_0^z(\mathrm{A}\rightarrow\mathrm{J}) + \frac{\mathcal{C}_0^z(\mathrm{A}\rightarrow\mathrm{J})}{kT}\right)f(\mathcal{E})\right] \tag{3}$$

$$\frac{A}{\mathcal{E}} \equiv \frac{A_L + A_R}{2\mathcal{E}} = \gamma\mathcal{D}_0^z(\mathrm{A}\rightarrow\mathrm{J})f(\mathcal{E}) \tag{4}$$

$$\frac{\Delta I'}{\mathcal{E}} = -\gamma_e\mu_B B\left[\mathcal{A}_1^z(\mathrm{J}\leftarrow\mathrm{A})\left(\frac{\partial\bar{f}(\mathcal{E})}{\partial\mathcal{E}}\right) + \left(\mathcal{B}_0^z(\mathrm{J}\leftarrow\mathrm{A}) + \frac{\mathcal{C}_0^z(\mathrm{J}\leftarrow\mathrm{A})}{kT}\right)\bar{f}(\mathcal{E})\right] \tag{5}$$

$$\frac{I}{\mathcal{E}} \equiv \frac{I_L + I_R}{\mathcal{E}} = 2\gamma_e\mathcal{D}_0^z(\mathrm{J}\leftarrow\mathrm{A})\bar{f}(\mathcal{E}) \tag{6}$$

(7) Piepho, S. B.; Schatz, P. N. *Group Theory in Spectroscopy with Applications to Magnetic Circular Dichroism*; Wiley: New York, 1983.

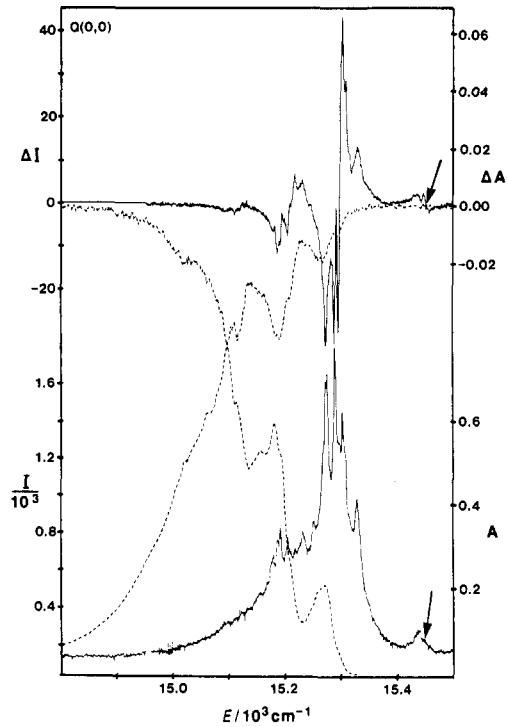

Figure 2. Detail of the Q(0,0) region. Units and nomenclature as in Figure 1. Spectral bandwidths are 0.3 nm for the emission (ΔI and I) and 0.15 nm for the absorption and MCD (A and ΔA). The lower vertical arrow designates the absorption shoulder at ~15 440 cm^{-1} due to a JT-active mode of frequency 154 cm^{-1}, and the upper arrow indicates the accompanying *negative* $\mathcal{A}$ term.

$\mathcal{E} = h\nu$ is the photon energy, γ and γ_e are collections of various constants that will cancel from the ratios of concern to us and μ_B and B are respectively the Bohr magneton and the magnetic induction in tesla. Superscript z designates a quantity orientationally averaged in the plane of the deposition window, and $f(\mathcal{E})$ and $\bar{f}(\mathcal{E})$ are respectively the line-shape function in absorption and emission. The parameters in eqs 5 and 6 are defined so that $\mathcal{A}_1(\mathrm{A}\leftarrow\mathrm{J}) \equiv \mathcal{A}_1(\mathrm{J}\rightarrow\mathrm{A})$ and so on.[7] Note that we follow the standard CPL convention and *define* the total luminescence as $I = I_L + I_R$ in contrast to the CD convention for the total absorbance, $A = (A_L + A_R)/2$.

In our present discussion we identify A with the ZnPc ground state ($^1A_{1g}$) and J with the Q state ($^1E_u^Q$) and assume that the flat absorbing and emitting ZnPc molecules are randomly oriented exclusively in planes parallel to the deposition window. We have previously shown that[1]

$$\mathcal{A}_1^z(^1A_{1g}\rightarrow{}^1E_u) = i\sum_{\lambda\lambda'}\langle{}^1E_u\lambda|L_z|{}^1E_u\lambda'\rangle\vec{k}\cdot\langle{}^1A_{1g}|\vec{m}|{}^1E_u\lambda\rangle \times \langle{}^1E_u\lambda'|\vec{m}|{}^1A_{1g}\rangle \tag{7}$$

$$\mathcal{B}_0^z(^1A_{1g}\rightarrow{}^1E_u^J) = 2\,\mathrm{Im}\left[\sum_{\lambda}\sum_{\substack{K\kappa\\(K\neq J)}}\frac{\langle{}^1E_u{}^J\lambda|L_z|{}^1E_u^K\kappa\rangle}{E_K - E_J}\vec{k}\cdot\langle{}^1A_{1g}|\vec{m}|{}^1E_u^J\lambda\rangle \times \langle{}^1E_u^K\kappa|\vec{m}|{}^1A_{1g}\rangle\right] \tag{8}$$

$$\mathcal{C}_0^z(^1A_{1g}\rightarrow{}^1E_u) = 0 \tag{9}$$

$$\mathcal{D}_0^z(^1A_{1g}\rightarrow{}^1E_u) = \frac{1}{2}\sum_{\lambda}[|\langle{}^1A_{1g}|m_x|{}^1E_u\lambda\rangle|^2 + |\langle{}^1A_{1g}|m_y|{}^1E_u\lambda\rangle|^2] \tag{10}$$

$\vec{L}$ and $\vec{m}$ designate the orbital angular momentum and electric dipole operators respectively, Im = imaginary part, $i = (-1)^{1/2}$, and all quantities are referenced to molecular axes (z is perpendicular to the molecular plane); $\vec{k}$ is a unit vector along z, E_K and E_J are the energies of the indicated electronic states, and in eq 8 we have assumed that only excited-state mixing is important.

Noting that[7]

$$|\langle A|m_{\mp 1}|J\rangle|^2 = |\langle J|m_{\pm 1}|A\rangle|^2 \tag{11}$$

where $m_{\pm 1} = \mp(m_x \pm im_y)/2^{1/2}$, we can readily relate the parameters in eqs 5 and 6 to those in eqs 3 and 4 with the results

$$\mathcal{A}_1^z({}^1A_{1g}\leftarrow{}^1E_u) = \frac{1}{2}\mathcal{A}_1^z({}^1A_{1g}\rightarrow{}^1E_u)$$

$$\mathcal{B}_0^z({}^1A_{1g}\leftarrow{}^1E_u) = -\frac{1}{2}\mathcal{B}_0^z({}^1A_{1g}\rightarrow{}^1E_u)$$

$$\mathcal{C}_0^z({}^1A_{1g}\leftarrow{}^1E_u) = \frac{1}{2}\mathcal{A}_1^z({}^1A_{1g}\rightarrow{}^1E_u)$$

$$\mathcal{D}_0^z({}^1A_{1g}\leftarrow{}^1E_u) = \frac{1}{2}\mathcal{D}_0^z({}^1A_{1g}\rightarrow{}^1E_u) \tag{12}$$

The factors of $^1/_2$ in eq 12 are a consequence of the double degeneracy of ^1E_u.

For the transition $^1A_{1g} \rightarrow {}^1E_u$, we expect $\mathcal{A}$ terms to dominate the MCD, and the MCD in the Q(0,0)-band region (Figure 2) *does* appear to show $\mathcal{A}$ terms. From eqs 7 and 10 we obtain[1]

$$\frac{\mathcal{A}_1^z({}^1A_{1g}\rightarrow{}^1E_u^J)}{\mathcal{D}_0^z({}^1A_{1g}\rightarrow{}^1E_u^J)} \equiv g_\parallel \tag{13}$$

$$g_\parallel = 2i\langle {}^1E_u^J x|L_z|{}^1E_u^J y\rangle \tag{14}$$

$\mathcal{A}_1^z/\mathcal{D}_0^z$ is therefore a direct measure of the orbital angular momentum of the excited state. The value of $g_\parallel$ can be obtained directly from the experimental data using the method of moments:[7,8]

$$g_\parallel \mu_B B = M_1/A_0 \tag{15}$$

where M_n is the nth MCD moment and A_n is the nth zero-field absorption moment obtained by numerical integration of the experimental data:

$$M_n = \int \left(\frac{\Delta A'}{\mathcal{E}}\right)(\mathcal{E} - \bar{\mathcal{E}})^n \, d\mathcal{E} \tag{16}$$

$$A_n = \int \left(\frac{A}{\mathcal{E}}\right)(\mathcal{E} - \bar{\mathcal{E}})^n \, d\mathcal{E} \tag{17}$$

$\bar{\mathcal{E}}$ is the band barycenter, defined by $A_1 = 0$: $\bar{\mathcal{E}} = \int A \, d\mathcal{E}/\int (A/\mathcal{E}) \, d\mathcal{E}$. It is clear by inspection (MCD in Figure 2) that the first MCD moment (M_1) is positive so that $g_\parallel$ must also be positive by eq 15.

According to eq 3, true $\mathcal{A}$ terms should show zero crossings at energies corresponding to absorption maxima. However, from close inspection of the data (Figure 2), we have previously found that the MCD actually exhibits maxima and minima at these energies.[1] This gives clear evidence that the Q state is split, presumably by the action of a crystal-field-stabilized Jahn–Teller (JT) effect.[1,2] By this we mean that the ^1E_u state is Jahn–Teller coupled to b_{1g} and/or b_{2g} modes in point group D_{4h} producing two identical potential surfaces of equal energy separated in b_{1g}/b_{2g} configuration space. Any environmental effect ("crystal field") that lowers the site symmetry from D_{4h} will in general shift the two potential surfaces by different amounts along the energy axis thereby removing the 2-fold vibronic degeneracy.[9] In that event, only $\mathcal{B}$ terms can appear in the MCD. If the splitting is not too large compared with the vibronic bandwidths, the $\mathcal{B}$ terms overlap to give the overall appearance of $\mathcal{A}$ terms—so-called pseudo-$\mathcal{A}$ terms.[7]

The integrations in eqs 16 and 17 must include the entire band envelope described by the excited-state basis set, i.e., Q(1,0) and Q(2,0) as well as Q(0,0). In that event eqs 13–15 continue to apply in the presence of first-order (in-state) Jahn–Teller (JT) and/or crystal field effects, no matter how complicated, because of the invariance of M_1/A_0 to unitary transformations on the excited-state manifold.[7] However, we have shown previously[1] that Q(2,0) arises in part from an additional electronic transition (Q′) which would invalidate the theoretical significance of such an integration. Therefore, before carrying out the numerical integrations of the experimental data, we deconvolute out the contribution of Q′ on the basis of our earlier vibronic simulation of Q(2,0)—see Figure 7 and section V.1 of ref 1. Then using eq 15, we obtain $g_\parallel = 3.2$.

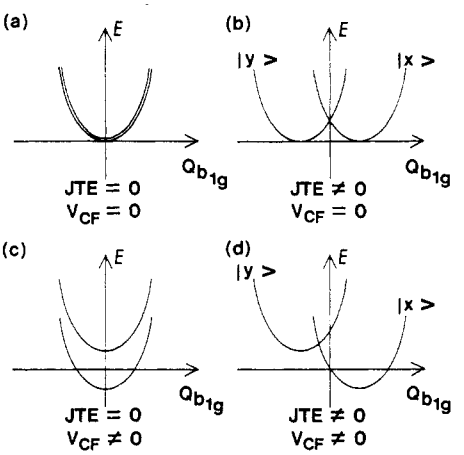

Figure 3. Schematic of the $^1E_u x$ and $^1E_u y$ potential surfaces in the absence and presence of Jahn–Teller (JT) and/or crystal field (CF) effects.

To discuss the emission spectra, we adopt a very simple model by assuming that a single JT-active mode and a crystal field *of the same symmetry* are operative. (The analysis is identical for a b_{1g} or b_{2g} mode, and we therefore arbitrarily assume that both the crystal field and JT perturbation belong to the b_{1g} irreducible representation of point group D_{4h}.) The JT effect splits the $|{}^1E_u^Q\rangle$ potential surface into $|{}^1E_u^Q x\rangle$ and $|{}^1E_u^Q y\rangle$ components along $Q_{b_{1g}}$, and the crystal field separates the components along the energy axis. This is depicted schematically in Figure 3, where we also show the separate effects (which are additive). We assume arbitrarily that $|{}^1E_u^Q x\rangle$ is lower in energy. (Our subsequent analysis is independent of this assumption.)

We start by assuming a zero JT effect so that the potential surfaces $|{}^1E_u^Q x\rangle$ and $|{}^1E_u^Q y\rangle$ *remain parallel* (Figure 3c). Then the Born–Oppenheimer and rigid shift approximations are justified, and eqs 3–6 remain valid. In addition, eq 15 continues to apply rigorously, as mentioned above. In the emission case, eqs 5 and 6 can now be written

$$\frac{\Delta I'}{\mathcal{E}} = -\gamma_e \mu_B B \sum_{\lambda=x,y} \delta_\lambda \mathcal{B}_0^z({}^1A_{1g}\leftarrow{}^1E_u^Q\lambda)\bar{f}_\lambda(\mathcal{E}) \tag{18}$$

$$\frac{I}{\mathcal{E}} = 2\gamma_e \sum_{\lambda=x,y} \delta_\lambda \mathcal{D}_0^z({}^1A_{1g}\leftarrow{}^1E_u^Q\lambda)\bar{f}_\lambda(\mathcal{E}) \tag{19}$$

where δ_λ is the fraction of the molecules in emitting state $|{}^1E_u^Q\lambda\rangle$.

We assume that field-induced mixing only between $^1E_u^Q x$ and $^1E_u^Q y$ is important in view of their small energy separation; we can use eqs 8 and 10 by identifying $^1E_u^J$ and $^1E_u^K$ with $^1E_u^Q x$ and $^1E_u^Q y$, respectively, and dropping the sums over K, κ, and λ. The results are

$$\mathcal{B}_0^z({}^1A_{1g}\leftarrow{}^1E_u^Q x) = -\mathcal{B}_0^z({}^1A_{1g}\leftarrow{}^1E_u^Q y) = -\mathcal{B}_0^z({}^1A_{1g}\rightarrow{}^1E_u^Q x)$$
$$= g_\parallel |\langle {}^1A_{1g}|m_x|{}^1E_u^Q x\rangle|^2/\Delta E \tag{20}$$

where $\Delta E \equiv E({}^1E_u^Q y) - E({}^1E_u^Q x)$ and

$$\mathcal{D}_0^z({}^1A_{1g}\rightarrow{}^1E_u^Q x) = \mathcal{D}_0^z({}^1A_{1g}\leftarrow{}^1E_u^Q x) = \mathcal{D}_0^z({}^1A_{1g}\leftarrow{}^1E_u^Q y)$$
$$= \frac{1}{2}|\langle {}^1A_{1g}|m_x|{}^1E_u^Q x\rangle|^2 \tag{21}$$

Using these results, eqs 18 and 19 become

(8) Stephens, P. J. In *Advances in Chemical Physics*; Prigogine, I., Rice, S. A., Eds.; Wiley: New York, 1976; Vol. 35, p 197.
(9) Canters, G. W. *J. Chem. Phys.* **1981**, *74*, 157.

$$\frac{\Delta I'}{\mathcal{E}} = \frac{-\gamma_e \mu_B B g_\parallel}{\Delta E}[\delta_x \bar{f}_x(\mathcal{E}) - \delta_y \bar{f}_y(\mathcal{E})]|\langle {}^1A_{1g}|m_x|{}^1E_u^Q x\rangle|^2 \quad (22)$$

$$\frac{I}{\mathcal{E}} = \gamma_e[\delta_x \bar{f}_x(\mathcal{E}) + \delta_y \bar{f}_y(\mathcal{E})]|\langle {}^1A_{1g}|m_x|{}^1E_u^Q x\rangle|^2 \quad (23)$$

If we assume $\delta_x \gg \delta_y$, i.e., $\Delta E \gg kT$, and recall (eq 13) that $g_\parallel > 0$, we see from eq 22 that the MCPL should be negative, as is observed. Note that this conclusion and eq 22 are independent of the assumed energy order of $|{}^1E_u^Q x\rangle$ and $|{}^1E_u^Q y\rangle$. Thus if the roles of x and y are interchanged, *both* ΔE and the term in brackets change sign, and we get the same result as before.

It is useful to examine eqs 22 and 23 in the limits $\Delta E \gg kT$ and $\Delta E \to 0$. In the former, $\delta_x = 1$, $\delta_y = 0$, and the results are obvious. In the latter, we note that to first order in ΔE, $\bar{f}_y(\mathcal{E}) = \bar{f}_x(\mathcal{E}) - (\partial \bar{f}_x(\mathcal{E})/\partial \mathcal{E})\Delta E$, $\delta_x = 1/2 + \Delta E/4kT$ and $\delta_y = 1 - \delta_x$, assuming a Boltzmann distribution between ${}^1E_u^Q x$ and ${}^1E_u^Q y$. Substituting these expressions into eqs 22 and 23, we obtain

$$\frac{\Delta I'}{\mathcal{E}} = \frac{-\gamma_e \mu_B B g_\parallel}{2}\left[\frac{\bar{f}_x(\mathcal{E})}{kT} + \frac{\partial \bar{f}_x(\mathcal{E})}{\partial \mathcal{E}}\right]|\langle {}^1A_{1g}|m_x|{}^1E_u^Q x\rangle|^2 \quad (24)$$

$$\frac{I}{\mathcal{E}} = \gamma_e \bar{f}_x(\mathcal{E})|\langle {}^1A_{1g}|m_x|{}^1E_u^Q x\rangle|^2 \quad (25)$$

These equations are consistent with eqs 5 and 6 when J and A in the latter are identified with ${}^1E_u^Q$ and ${}^1A_{1g}$, respectively, as may be confirmed by using eqs 11 and 12. (Equation 24 does not contain a $\mathcal{B}$ term because we have neglected out-of-state mixing.)

Let us now turn on the JT effect in $Q_{b_{1g}}$. This causes a fundamental change because the two potential surfaces separate along $Q_{b_{1g}}$ and thus are no longer parallel (Figure 3d). Using the experimental data, we may roughly estimate the magnitude of this separation (and thus the strength of the JT coupling) as follows.

First we note that we are in the regime $\Delta E \gg kT$. This is ascertained by a careful examination of the data which show that the peaks in the MCPL and TL (though less well resolved) coincide with *minima* in the MCD. In the opposite limit, the first term in eq 24 would dominate and the TL and MCPL peaks would more or less coincide with the *zero crossings* of the MCD. Thus eqs 22 and 23 are the relevant starting equations with $\delta_x \approx 1$, $\delta_y \approx 0$. However, eq 22 must now be modified because the vibrational functions on the potential surfaces $|{}^1E_u^Q x\rangle$ and $|{}^1E_u^Q y\rangle$ are no longer mutually orthonormal, i.e., $\langle v_x|v_y\rangle \equiv \gamma_{v_x v_y} \neq \delta_{v_x v_y}$ where v_x and v_y designate the vibrational quantum numbers of harmonic oscillator functions on the respective surfaces. As a consequence, the right-hand side of eq 20 will now contain mixing terms between $|0_x\rangle$ and *all* $|v_y\rangle$. Thus eq 22 becomes (with $\delta_x = 1$)

$$\frac{\Delta I'}{\mathcal{E}} = -\gamma_e \mu_B B g_\parallel \bar{f}_x(\mathcal{E})|\langle {}^1A_{1g}|m_x|{}^1E_u^Q x\rangle|^2 \sum_{v_y=0}^{\infty} \frac{\gamma_{0v_y}^2}{\Delta E + v_y h\nu} \quad (26)$$

where ν is the JT-active fundamental frequency. If we now integrate eqs 23 and 26 over the entire band (i.e., determine the zeroth moments $M_0^\epsilon \equiv \int(\Delta I'/\mathcal{E})\, d\mathcal{E}$ and $A_0^\epsilon \equiv \int(I/\mathcal{E}\, d\mathcal{E})$, we obtain

$$\frac{M_0^\epsilon}{A_0^\epsilon} = -\mu_B B g_\parallel \sum_{v_y=0}^{\infty} \frac{\gamma_{0v_y}^2}{\Delta E + v_y h\nu} \quad (27)$$

If we now divide by the MCD moment ratio M_1/A_0 (eq 15), we obtain

$$\frac{M_0^\epsilon/A_0^\epsilon}{M_1/A_0} = -\sum_{v_y=0}^{\infty} \frac{\gamma_{0v_y}^2}{\Delta E + v_y h\nu} \quad (28)$$

By numerically integrating the emission data, we determine $M_0^\epsilon/A_0^\epsilon$, and combining this with the corresponding value of M_1/A_0 mentioned above, we obtain the experimental value, $-0.01 \pm 20\%$ for the left-hand side of eq 28. In determining $M_0^\epsilon/A_0^\epsilon$ we again (as with M_1/A_0) have the complication of a spurious contribution in the overtone region, in this case due to a trace of H_2Pc impurity as mentioned earlier. It is not possible to deconvolute this contribution, so we have simply included it in our numerical integrations. This cannot cause serious error because the contribution of the overtone region to the total area is relatively small (Figure 1). Because the $|{}^1E_u^Q x\rangle$ and $|{}^1E_u^Q y\rangle$ components are separated by ~ 1000 cm^{-1} in H_2Pc/Ar,[10] and by only about 40 cm^{-1} in ZnPc/Ar (see below), we expect $\Delta I'/I$ to be much smaller in H_2Pc than in ZnPc so that our procedure will give a lower limit for $M_0^\epsilon/A_0^\epsilon$.

The right-hand side of eq 28 depends on ΔE, $h\nu$, and λ, the latter being the separation of the two potential minima along $Q_{b_{1g}}$—see Figure 3b. We can only estimate an average value for ΔE, since this quantity varies somewhat from site to site, and it is also possible that additional unresolved sites are present. However, analysis of the site splittings in both the present and earlier MCD and absorption data[1] for the region of strong emission ($\sim 14\,900$–$15\,300$ cm^{-1}) consistently suggests values for ΔE in the range $\sim 40 \pm 10$ cm^{-1}.

The single most important JT-active mode with about 5% of the intensity of the Q(0,0) envelope has $h\nu = 154$ cm^{-1} (ref 1, Table II); its location is shown by the vertical arrows in Figure 2. The fact that it is JT-active, i.e., that it is of symmetry b_{1g} or b_{2g}, is unambiguously demonstrated[1] by the fact that it gives a *negative* $\mathcal{A}$ term in the MCD.

The γ_{0v_y} are overlap integrals between displaced harmonic oscillators. They are a function only of λ and are readily evaluated.[11] Since the JT effect is small in the present case, the right-hand side of eq 28 converges rapidly. Using $\Delta E = 40$ cm^{-1} and $h\nu = 154$ cm^{-1}, we find by trial and error that $\lambda = 1.57 \pm 0.2$. From elementary considerations it follows that the intersection point of the two curves in Figure 3b occurs at $E_{JT} = (1/8)\lambda^2 h\nu$. Using $\lambda = 1.57$, we obtain $E_{JT} \approx 47$ cm^{-1}. We may simplify this treatment further without much loss of accuracy by retaining only the $v_y = 0$ term on the right-hand side of eq 28. Then solving, we obtain $\gamma_{00} = 0.63$.

It is easy to show that[11]

$$\gamma_{00} = \langle 0_x|0_y\rangle = \exp(-\lambda^2/4) \quad (29)$$

and solving we obtain $\lambda = 1.35$ ($E_{JT} \approx 35$ cm^{-1}). γ_{00} is the well-known Ham effect factor[12] which quenches the orbital angular momentum of the no-phonon line as the potential surfaces separate along the JT-active coordinate.

Our values for ΔE, ν, and λ (~ 40 cm^{-1}, 154 cm^{-1}, and 1.57) are close to those deduced for CdTBP (TBP = tetrabenzoporphyrin) in the Shpol'skii host *n*-octane,[13] namely, ~ 30 cm^{-1}, 150 cm^{-1}, and 1.27. However, it should be emphasized that our λ is really an effective parameter, and its magnitude is necessarily an upper limit because we have attributed all of the activity to a single JT-active mode whereas a number of such modes are actually active (ref. 1, Table II). Furthermore, if we assume a more complex relation between $\hat{H}_{JT}$ and $\hat{H}_{CF}$, for example, that each belongs to a different irreducible representation (b_{1g} and b_{2g}) or most generally that each contains contributions from both, then the simple picture (Figure 3) is no longer applicable and the JT and crystal field effects may partly quench each other.[9] In that event, the right-hand side of eq 27 will obviously assume a more complex form. It might well be possible to derive an analytical result for this case using perturbation theory.

One of the more striking features of Figure 2 is the red shift of the emission relative to the absorption. We are confident that virtually all of the bands below $\sim 15\,400$ cm^{-1} in the absorption spectrum are zero-phonon lines and that the structure in Figure 2 is due to the presence of inequivalent sites.[1,2] The red shift cannot therefore be a result of intramolecular vibrational relaxation. Nor can it be explained by reabsorption of emitted radiation. If we assume a homogeneous matrix, then the strongest absorption in

(10) Bondybey, V. E.; English, J. H. *J. Am. Chem. Soc.* **1979**, *101*, 3446.
(11) See, for example: Fulton, R. L.; Gouterman, M. *J. Chem. Phys.* **1961**, *35*, 1059, Appendix IV.
(12) See, for example: Englman, R. *The Jahn-Teller Effect in Molecules and Crystals*; Wiley: New York, 1972.
(13) Platenkamp, R. J.; Canters, G. W. *J. Phys. Chem.* **1981**, *85*, 56.

the Q(0,0) region (~0.8 OD unit, Figure 2) can account for only ~60% attenuation, which cannot possibly explain the fact that the strongest emission occurs at ~15 100 cm^{-1} and corresponds to sites that are only weakly discernible in absorption.

The relative intensity of the emission bands is independent of excitation frequency, and we conclude that the red shift of the emission *must* result from intermolecular energy transfer between inequivalent sites. The lower energy sites are traps for the excitations and hence show strongly enhanced emission. In a similar manner, the presence of small amounts of H_2Pc gives rise to zero-phonon emission bands between 14 200 and 14 700 cm^{-1} (Figure 1) even though the corresponding absorption bands are too weak to be observed.

We note that the experimental value (3.2) of $g_\parallel$ determined in this work using eq 15 is appreciably lower than our usual value of 4.2,[1] implying that only partial orientation parallel to the deposition window occurs. (Application of eq 15 to a completely random sample would give an effective $g_\parallel \approx 2.1$.[1]) This partial loss of orientation is almost certainly due to the fact that we used a sapphire deposition window in the present work rather than a LiF deposition window.[1] Among other differences, sapphire has a far higher heat conductivity at liquid He temperatures. We emphasize that the crucial ratio for estimating the Ham effect quenching (left-hand side of eq 28) is independent of the degree of selective orientation.

Conclusions

Our results confirm that the $^1E_u^Q$ excited state of ZnPc/Ar is split due to both crystal field and Jahn–Teller effects. Thus the fact that the MCPL is dominated by single-signed $\mathcal{B}$ terms means that $^1E_u^Q$ is split along the energy axis (crystal field), and the quenching of its orbital angular momentum means that it is also split along b_{1g} and/or b_{2g} coordinates (JT splitting). The zero-phonon luminescence is also markedly shifted to lower energy with respect to the absorption thus strongly implying energy transfer between inequivalent sites in the matrix.

Our results also strongly imply that relaxation between the two split components of $^1E_u^Q$ is fast compared to the lifetime of the state since the MCPL (and TL) peaks line up with the negative lobes in the MCD showing that emission is predominantly from the lower component of $^1E_u^Q$. This also suggests that our estimate of λ (and thus of E_{JT}) is an upper limit since the presence of multiple sites make the spectra sufficiently complex that we cannot completely preclude the presence of some emission from the upper component of $^1E_u^Q$ (although we see no evidence of it). Such emission would lower the zeroth MCPL moment, M_0 (see eq 22), and would be indistinguishable from JT coupling in our treatment. In contrast to our result in an Ar matrix, it is reported[2] that relaxation between the two no-phonon components of $^1E_u^Q$ of ZnPc in a hydrocarbon (Shpol'skii) matrix at 4.2 K is slow compared to the excited-state lifetime.

We also note that our interpretation has been limited in the present case by the occurrence of multiple, overlapping sites and by spurious contributions in the sidebands which limit the accuracy of our numerical integrations (moment analyses). However, we believe this work demonstrates the considerable potential of MCPL/TL measurements to provide detailed information about vibronic coupling in excited (emitting) states in matrix-isolated species. In other systems, we may anticipate cleaner spectra that would justify a more detailed theoretical treatment allowing for the activity of several JT modes and the presence of a more complex crystal field. It would also be very interesting to study emitting states that are not directly accessible in absorption. We shall report in future work an MCPL study of Zn tetrabenzoporphyrin/Ar. This sytem is known to emit from the Q state, its triplet analogue and from the singlet B state,[14,15] and its MCD spectrum shows very sharp features approaching a width of ~4 cm^{-1} in the Q band.[15]

Acknowledgment. This work was supported by the National Science Foundation under Grants CHE8215815 (awarded to F. S. Richardson), CHE8700754, and CHE8902456.

Registry No. ZnPc, 14320-04-8; Ar, 7440-37-1.

(14) Bajema, L.; Gouterman, M.; Rose, C. B. *J. Mol. Spectrosc.* **1971**, *39*, 421.

(15) VanCott, T. C. Ph.D. Thesis, University of Virginia, Charlottesville, VA, 1989.